

# Hot rolling: mechanical, microstructural, modeling, simulation for both ferrous and light metals

H.J. McQueen, P. Leo

*The dimensions, speed and complexity of rolling mills have been advancing with understanding of the mechanics and augmented calculating power. However, the metallurgical mechanisms both during the passes and between them are significant for stresses, defect avoidance and product properties. With facile ability to examine microstructures at end of any pass or interval, physical simulation of multistage rolling has been achieved in torsion, as well as in plane strain compression; while the former excels in number of passes and total strains  $\epsilon$ , the latter can provide texture information. However, for product mechanical properties, torsion only permits hardness of the surface layer while plane strain specimens would permit tension or bending.*

*From dependencies on strain, strain rate and temperature  $T$  of stresses and microstructure for Al alloys, C/HSLA/tool steels and ferritic/austenitic alloys, the dependence on microstructural mechanisms during straining and unloaded intervals can be clearly defined and related to rolling forces and power demands. The effects of solute, particles and lattice dependent dislocation mobility can provide understanding of broad range of industrial requirements for product properties. For C/HSLA steels, there is the added complexity of adding a cooling procedure that ensures planned phase transformations. For Al alloys and stainless steels, the final cooling schedule can be arranged to provide prevention of, or any degree of static recrystallization, with control of grain size and degree of isotropy. The multistage rolling simulations combined with examination by optical microscopy OM, TEM and SEM-OIM improve process controls and product properties.*

**Keywords:** Al alloys - Hot rolling Al alloys - Hot rolling stainless steels - hot rolling C/HSLA/tool steels - Hot torsion rolling simulations - Laboratory rolling - Microstructures in hot rolling Al alloys/steels - TMP Al alloys/steels

## INTRODUCTION: HISTORY, ROLLING, MICROSTRUCTURE

A historical review shows that hot forging of steel has been employed for centuries with the defining effect by human strength and skill, i.e. long before rolling [1-4]. Moreover, hot rolling was developed for ferrous alloys long before cold rolling was introduced but the latter advanced rapidly because of no requirement to maintain temperature  $T$  in a narrow time program. The microstructural changes in cold working were well defined by 1950, whereas very little had been clarified in the hot working range ( $>0.5 T_m$

melting K, strain rate  $\dot{\epsilon} = 10^{-2}$ - $10^{+2}$ s $^{-1}$ ) [4,5]. The historical development of roll processing is presented followed by an analysis of flow strength and ductility dependence on  $T$  and  $\dot{\epsilon}$  in the two domains. The development of properties and microstructures in single stage and in multistage straining is then examined for Al alloys,  $\alpha$ -Fe alloys and  $\gamma$ -Fe alloys. In normal rolling schedules, dynamic recovery [DRV] is the principle softening mechanisms of almost all metals [5-16]; the exception is dynamic recrystallization [DRX] in very large passes and high temperatures [4-11,17,18], as occurs in planetary mill rolling of austenitic stainless steels. In austenitic steels (Ni, Cu also), there is usually static recrystallization (SRX) between passes with finer grain sizes, as temperature falls in preceding pass; the exception is stainless steels, where SRX would decline to less than 10% by 1000°C. In Al alloys and ferritic steels SRX might occur after the first 3 - 6 passes, but not after that unless the inter-pass time is extended in mid-schedule (8-10 of 17 passes), aimed at grain refinement and texture change for final isotropic properties.

The wrought iron era, (1780 - 1870) developed the hot working of austenitic iron ( $\gamma$ -Fe) linked to gradual build up of product size by hot pressure welding of 50 kg puddled

**H.J. McQUEEN**

*Mech. Eng., Concordia Univ., Montreal, H3G 1M8,  
Canada, (McQUEEN@encs.concordia.ca)*

**P. Leo**

*Innovation Eng Dept, Univ. of Salento,  
73100, Lecce, Italy  
(paola.leo@unisalento.it)*

Paper presented at the Int. Conf. ROLLING 2013, Venice  
10-12 June 2013

bars [1,2,19,20]. Forging capably produced long drive shafts for steam ships, but was also extremely important for sheets to go to slitting mills (~1600). Sheet productivity was enhanced by folding the sheet and pack rolling up to 8 layers. Rolling was limited by slow, manual handling and reductions, achievable without difficult reheating of the elongated material. The 3-high mill (~1830) caused a major improvement especially for bars, angles and T-shapes. The change to steel ingots (~1860) required little change in the heating pattern with preheats of about 1100 °C, since finishing had to be completed before transformation started at 900 - 800 °C in low to medium C steels [2,3,19]. A serious constraint was avoidance of overheating to liquefaction at grain boundaries (GB) that led to burning of the C and segregation of brittle products. The early small steel ingots could be accommodated on the largest WI rolling mills but for the more productive large ingots, much larger blooming mills were needed. This change was adopted widely in the USA while breakdown by forging remained the most common practice in Britain despite its lower productivity.

The larger initial work piece gave rise to a wide variety of developments. For longer steel bars, the looping mill was introduced where the emerging end of the bar was caught by hand tongs and swung to the next stand; later, mechanical guide rolls rotated products 90° axially to improve product symmetry. For plates/sheets, mechanical tables were developed and reversing mills (~1860), first through clutching between two steam engines running in opposite directions and later through use of locomotive engines with reversal valves and no condensers (solution came only with electric motors) [3,19,20]. When sheet/strip lengths were limited by cooling, the tandem continuous mill was introduced (1862-69) where four or more stands in succession were run at higher speeds to accept the accelerating sheet. The large ingots made it feasible to progress into production of large structural shapes such as I and H beams [19]. Vertical axis rolls were then needed for lateral dimensional control; much later, the universal mill provided integrated rolling on two axes.

## SCIENTIFIC STUDY OF HOT AND COLD WORKING, ROLLING

Cold rolling involved problems of marked rise in strength (roll forces) and decrease in ductility (edge cracking) that could be avoided by annealing before a definable strain for each alloy. These characteristics could easily be studied by taking specimens from production at roll speed after any stage without concern for alteration, since not hot. Moreover, satisfactory tests could be carried out on tension/compression machines at  $\dot{\epsilon} \approx 10^{-3} \text{s}^{-1}$  in ambient T conditions. Consequently, between 1900 and 1950, the dependence of strength on reduction was established for most existing alloys. The grain structure changes in straining and in annealing were easily observed, notably by the formation of new, soft equiaxed grains, i.e., static

recrystallization (SRX). Through optical microscopy and x-ray diffraction, occurrence of slip relative to crystal orientation was defined. The relatively low flow stresses were explained about 1934, on through weakening by the motion of thread-like lattice defects of dislocations; this kindled research enthusiasm, yet no clear observations of dislocations for two decades [10-12,21]. The low-stacking fault energy in  $\gamma$ -Fe ( $\gamma$ -SS, stainless) expedites SRX by diminishing dislocation mobility and hence static recovery (SRV). In annealing, SRX was studied over a wide T range to determine the activation energy and dependence on prior  $\epsilon$  for most industrial alloys.

Despite many similarities in external features during processing, hot working was experimentally much different. Getting unaltered samples from hot industrial products was difficult since they could not be quenched to prevent change. Conducting tests on laboratory scale suffered from inability to attain the high industrial strain rates  $\dot{\epsilon}$ , and to match the T variation with time or strain [22-4]. It was only about 1965 that fast electronic equipment became able to record T from a thermocouple imbedded in the center of a 25 mm plate preheated in the range 300-1000 °C, as it passed directly from the furnace through cold or heated rolls rotating to give  $\dot{\epsilon} = 20/\text{s}$  for  $\epsilon = 2.3$  (90% reduction in one pass) (Figure 1) [25,26]. Even when quenched by dropping into chilled brine, Cu and Ni specimens exhibited SRX except for the final centimeter of the strip with elongated grains (no DRX, due to high  $\dot{\epsilon}$ ); in contrast, Al showed no SRX. The above were confirmed on a large mill [27,28] with addition of  $\gamma$ -SS,  $\Sigma\epsilon = 2.3$  in which either no SRX took place or complete SRX [9,27]; the textures in both were of Al/Cu type [28].

Hot rolling in the laboratory, while having deficiencies, often provided significant information as long as the shortcomings are kept in mind. In addition to single stage tests, multistage can be achieved notably with furnaces on each side of the mill. Ingenuity over years of research, studies were made of the effects at hot-work T and  $\dot{\epsilon}$  on SRX extent and grain size of  $\gamma$ -rolled C and HSLA steels [29]. Moreover, for studying transformations (indicated by magnetic changes), T and  $\dot{\epsilon}$  impact was determined on nucleation density of ferrite grains and on the time-temperature-transformations to varied microstructures through continuous magnetic evolution in liquid tin, coupled to sequential hardness and microstructures [29-34], also on transformation of tool and rail steels [35,36]. Multistage laboratory rolling with declining  $T_i$  constant  $\dot{\epsilon}_i$  of 3000 Al alloys showed that the subgrain size at the end of a pass decreased with following  $T_i$  and the increase in size was less during the interval, becoming unnoticeable at lower  $T_i$  [37,38].

In Sheffield multistage rolling research on 3014 alloy, a laboratory mill (automated reversing and screw-down recommended) employed tube furnaces at each side on movable frames with spring mounting so tubes could reposition easily for specimen distortion or deflection [39]. The specimen has a long imbedded thermocouple and flexible wires at both ends for manipulation by two

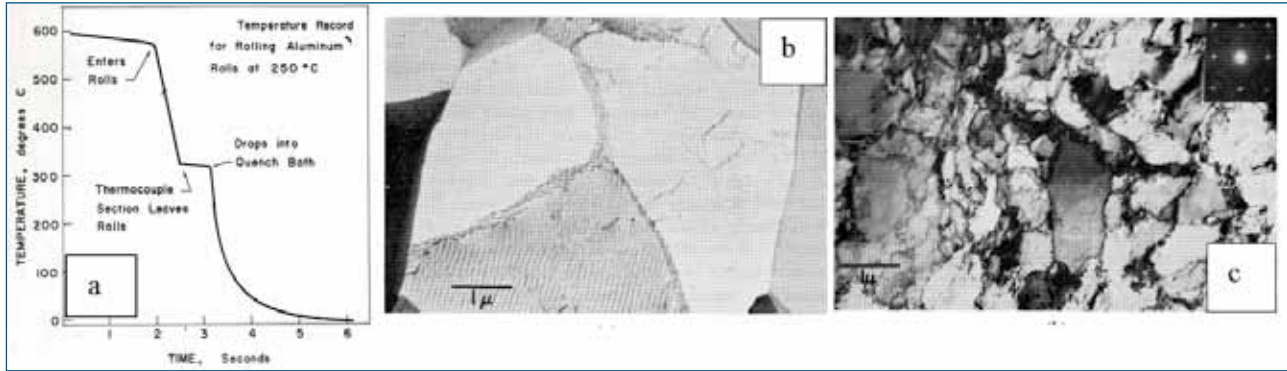


**Fig. 1 - Rolling from  $0.95 T_M$  on rolls at  $250^\circ\text{C}$  to 90% reduction in one pass, gives exit at  $0.65 T_M$ : a) T profile, imbedded thermocouple; b, c) TEM of: b) Al ( $340^\circ\text{C}$ ) and c) Ni ( $840^\circ\text{C}$ ) similar to  $\gamma\text{-Fe}$ , [25]. In comparable tests in 3 passes on a larger mill, 316 stainless had classic Al-Cu texture and an annealing cube texture [27].**

Fig. 1 - Laminazione da  $0,95 T_M$  su rulli riscaldati a  $250^\circ\text{C}$  con una riduzione di spessore del 90% in una sola passata e T di uscita del laminato pari  $0.65 T_M$ : a) profilo di T nel laminato rilevato da una termocoppia interna; micrografie TEM di: b) Al ( $340^\circ\text{C}$ ) e c), Ni ( $840^\circ\text{C}$ ) microstruttura simile a quello di un acciaio austenitico[25]. In test analoghi in 3 passate su un laminatoio più grande, l'acciaio 316 ha esibito la classica tessitura Al-Cu [27]

assistants. During the 14-break-down passes at 470 to  $430^\circ\text{C}$ , with intervals of 20 - 100 s that could be varied, the SRX decreases from surface to center and increases with rising pass number in agreement with single-valued constitutive constants. The constituent particle size was uniform across the section if the slab was air cooled from homogenization; in the rolling, constituent particle fracture spread from surface to central regions, as pass number rose. Texture developed as in industrial slabs [39].

## ALUMINUM & STEEL: COMMON HOT WORKABILITY (STEEL TRANSFORMATION)

At first glance, there is a large difference in the industrial hot processing conditions for alloys of Al [6-8,40] and those of Fe [5-10,40] in terms of T and forces; however at a common homologous  $T_H$  (i.e.  $0.7 T_M$  melting K: Al  $380^\circ\text{C}$ , Fe  $1000^\circ\text{C}$ ), there are many similarities in the mechanisms and in the flow curves that, in combination with the contrasts, improve the understanding. Al alloys and  $\gamma\text{-Fe}$  alloys are face-centered-cubic but the iron has a low-stacking fault energy [4,7-10,41-46], so dislocations are less able to undergo DRV in the 300 series stainless steels that is even more difficult due to solute. The TEM substructures can be observed both in Al alloys, [7-10,12,15,25,26,40,47] where low dislocation density delays nucleation, and in 300 stainless, where solute slows down nucleation; the subgrain sizes are very different yet vary with Z and  $\sigma$  in the same manner. Between these extremes lie the DRV levels in Al-Mg alloys ( $\sigma_s \gg$  Al) [48] and in C/HSLA steels ( $\sigma_s \ll$  stainless) ( $\gamma\text{-Fe}$  to  $\alpha\text{-Fe}$  reaction eliminates SGB in softer C steels) [6,7,29-34,47,49,50]. In body-centered-cubic  $\alpha\text{-Fe}$  and Al, the levels of DRV at the same  $T_H$  are fairly similar [6-9,41,51-58]. In consequence, Al alloys and  $\alpha\text{-Fe}$  have similar resistance to static and dynamic recrystallization (SRX and DRX). The substructures observable in stainless

steels are important for understanding those in C steels (at some  $100\text{-}200^\circ\text{C}$  lower T); substructure causes increased nucleation of ferrite in pancaked  $\gamma$  grains in controlled rolling [5,9,30-34,59,60]. Similar DRX in  $\gamma\text{-Fe}$  and in Ni provide greater insights [9,25,27,61].

The constitutive and microstructural equations for Al alloys and steels (C/HSLA, tool,  $\alpha$ - or  $\gamma$ -stainless) have the same form and the constants increase with alloying in a similar manner [47,60,62]:

$$A \sinh(\alpha \sigma_s)^n = \dot{\epsilon} \exp(Q_{HW}/RT) = Z$$

$$d_s = a + b Z^p$$

$$D_s = c + d Z^q$$

where the constants A,  $\alpha$  R(gas), a, b, c, p, q are constants; Z is Zener-Hollomon parameter containing control variables T and  $\dot{\epsilon}$  [43-47,51-54,57,58,60,61].

The first successful machine for constant  $\dot{\epsilon}$  (about 1950) was the compressive cam plastometer that required a separate cam at a given  $\dot{\epsilon}$  for a single specimen height; although rates of  $10^{-2}$  to  $10^{+2}$  could be attained, only a handful of such expensive machines with limited flexibility were built [22,24,63]. In creep testing about 1940, cams, lever arms increased the rate of pulling to give constant  $\dot{\epsilon}$  for specimens in tube atmosphere-controlled furnaces; these had been easy to construct because of the low  $\dot{\epsilon}$ . About 1960, the hot torsion machine (like a lathe with one and fixed in load cell) was developed that had considerable flexibility in T,  $\dot{\epsilon}$  and  $\epsilon$  (even to true  $\epsilon \approx 130$ ) (Figure 2) [23,24,49,50,61]. Specimen examinations posed difficulties due to an  $\dot{\epsilon}$  and  $\epsilon$  gradient with radius that required careful metallography and hardness tests only in a selected, narrow radial range for a given  $\dot{\epsilon}$  [24,40,49,50]. It was only in the 1970's that electronic motion measurements and control systems on

**Fig. 2 - Torsion testing at constant  $T$ , showing continuous (dashed) and multistage tests  $\epsilon_i = 0.2$ ,  $900^\circ\text{C}$ ,  $0.1\text{ s}^{-1}$ : a) C steel, 70-100% softening and b,c) Nb steel; c) 10-30% softening, but b) 10-40% at  $950^\circ\text{C}$  and c) much higher, 50-85% for  $\epsilon_i = 0.4$  at  $\dot{\epsilon} = 1.0\text{ s}^{-1}$  [65,66,70]. When the conditions for the Nb steel are altered to  $950^\circ\text{C}$ ,  $1.0\text{ s}^{-1}$   $\epsilon_i = 0.4$ , there is  $90^\circ$  softening in each interval of 20 s [65,70]. In simulation of a reversing hot mill for the Nb steel while in the coil box for 150 s, the softening was  $>100\%$  at  $1000^\circ\text{C}$ , 70-80% at  $900^\circ\text{C}$  and 40-50% at  $800^\circ\text{C}$  [70].**

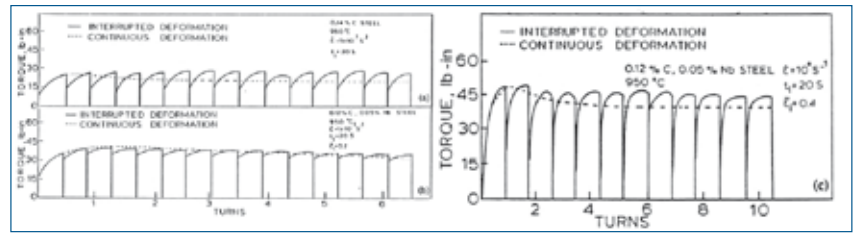


*Fig. 2 - Test di torsione continuo (linea tratteggiata) e multistadio (linea continua) con  $\epsilon_i = 0.2$ ,  $T = 950^\circ\text{C}$  e  $\dot{\epsilon} = 0.1\text{ s}^{-1}$  (a, b) e  $\epsilon_i = 0.4$ ,  $950^\circ\text{C}$ ,  $10\text{ s}^{-1}$  (c). L'acciaio al carbonio esibisce grado di softening pari al 70-100% (a), l'acciaio al Niobio pari al 10-30% (b) e fino al 50-85% se  $\epsilon_i = 0.4$  e  $\dot{\epsilon} = 1.0\text{ s}^{-1}$  [65,66,70]. Per  $\dot{\epsilon} = 10\text{ s}^{-1}$  e  $\epsilon_i = 0.4$ , il grado softening aumenta fino al 90% in ogni intervallo di 20s [65,70] (c).*

commercial tension/compression machines could vary the rate of screw rotations fast enough to provide constant  $\dot{\epsilon}$ . It still required quite complex equipment to provide furnaces with controlled atmospheres or vacuums and devices to transfer specimens into quenchants in less than 3 s. The Gleeble™ hydraulic compression machine with specimen resistance-heating provided good ranges of  $T$ ,  $\epsilon$  and  $\dot{\epsilon}$  as well as rapid quenching [22,24,64].

Torsion tests on C/HSLA austenites (as on Ni alloys [61]) showed the occurrence of a peak that was at lower  $\epsilon_p$  and  $\sigma_p$  for high  $T$  and lower  $\dot{\epsilon}$  isothermal simulations of a reversing mill showed complete SRX in coil boxes even for HSLA steels [49,50,65,66]. Two stage isothermal tests with interruptions at selected  $\epsilon$  of various types and times were able to measure the extent of SRV/SRX:

$$\text{Fractional Softening FS} = \frac{\{\sigma_{(\text{MI, MAX. BEFORE INTERVAL})} - \sigma_{(\text{RELOAD R}(i+1))}\}}{\{\sigma_{\text{MI}} - \sigma_{(\text{YI INITIAL YIELD})}\}}$$

and of alloying-element precipitation in order to guide selection of conditions for controlled rolling [29,49,50,67-70]. Optical microscopy in Cu, Ni and 300 stainless steels confirmed attainment by  $\sigma_p$  of about 30% dynamic recrystallization (DRX) and by its completion for  $\epsilon > \epsilon_s$ , a steady state plateau ( $\sigma_s$ ,  $\dot{\epsilon}$ ) with distributed repetition of DRX. Planetary mill modeling of stainless steels indicated that DRX continued successively under each small planet roller (slightly rising  $\dot{\epsilon}$ ,  $\sigma_s \sim 1100^\circ\text{C}$ ) that maintained a low force and high ductility [71]. Torsion of ferritic stainless steel exhibited attainment of a plateau without a peak and elongation of the grains with a presence of subgrains [51-55,72]. At very high strains because the elongated grain aspect disappeared, DRX was also suggested [70] but later work on Al indicated that the low  $\sigma_s$  and very high ductility were due to DRV [11,12,16,73].

In Al after 1955 a new etching/anodizing technique for polarized optical microscopy (POM) showed that both hot rolling and extrusion produced elongated grains with subgrains that were quite stable at the finishing  $T$ , although static recrystallization SRX could be induced by annealing (more quickly above the deformation  $T_p$ )

[25,26,40,63]. The application of the newly developed transmission electron microscopy (TEM) to extrusions and cam plastometer (constant  $\dot{\epsilon}$  and  $T$ ) specimens confirmed that the subgrain boundaries SGB were composed of fairly simple dislocation networks; the spacings  $d_s$  in steady state of the SGB and of the dislocations composing them were larger, as  $T$  increased and  $\dot{\epsilon}$  and  $\sigma$  decreased (Figure 1) [11,16,25,26,40,63]. At high strains (rising from 5 to 60, as grain size increased), the grain boundaries GB became serrated (corrugated) due to surface energy balancing with the SGB and became difficult to distinguish; this was initially called geometric DRX (although no nucleation) but recently better renamed grain-defining gDRV, grains (diameter  $D$ ) never became thinner than  $\sim d_s$  [7-9,11,12,14,16,21,73].

## ALUMINUM ALLOY MULTISTAGE SIMULATIONS

Since the SGB produced by hot working in Al were quite stable, they were observed by POM, TEM, SEM-EBS and OIM to determine the dependence on  $T$ ,  $\dot{\epsilon}$  and  $\epsilon$  of size  $d_s$  and of dislocation spacing in the walls and interiors of subgrains. The resistance to SRV and SRX was studied to see how processing might be manipulated to enhance either strength or ductility. Such effects on service properties were of consequence, notably in extrusion where the dislocation density increased towards the surface and SRX there resulted in marked loss in section strength [74-77]. The effects of impurities, of solutes and of precipitates were examined. In precipitation hardening alloys, working of solution treated billets in the range 200 to  $300^\circ\text{C}$  enhanced rapid formation of fine particles on the dislocations leading to high peak stress in torsion (initial pressure in extrusion) and possible fracture before coarsening allowed DRV to resume elimination of dislocations and restore ductility [76,78,79].

In Al-0.6Fe or Al-0.5Fe-0.5Co wire alloys the particle size had to be reduced and distribution uniformized by rapid solidification in a Properize Wheel and in the subsequent rolling in a continuous multi-stage rod mill (Figure 3) [80-83]. The right balance of size and distribution uniformity

**Fig. 3 - Multistage torsion tests on recrystallized Al-0.65Fe with  $T$  declining progressively (during intervals) from 500 to 300 °C at  $\dot{\epsilon} = 0.1 s^{-1}$ : a)  $\epsilon_i = 0.2$ ,  $t_i = 60$  s; and b) 0.4, 120 s (rod mill exit 35 MPa at 384 °C; isothermal continuous 400 °C,  $\sigma_s = 80$  MPa, in absence of SRV intervals [86].**

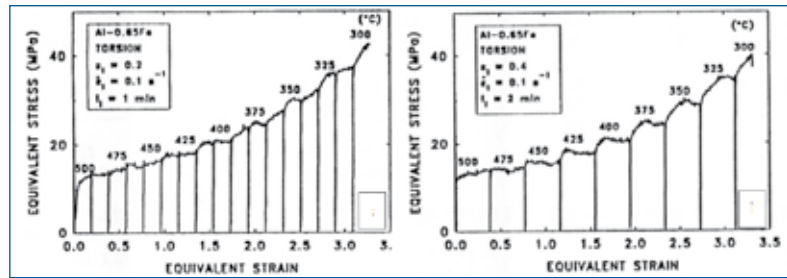


*Fig. 3 - Test di torsione multistadio su lega*

*Al-0,65Fe ricristallizzata, a  $T$  che decrescono progressivamente durante gli intervalli da 500 a 300 °C e  $\epsilon_i = 0.2$ ,  $t_i = 60$  s (a);  $\epsilon_i = 0.4$ ,  $t_i = 120$  s (b) (a causa del recupero, i valori di snervamento di ogni stadio, risultano sempre inferiori agli sforzi massimi dello stadio precedente ma superiori ai valori di snervamento di prove continue isoterme)*

of Al<sub>3</sub>Fe would provide ductility and stable strengthening in wire drawing. Finally, annealing had to provide conductivity and ease of handling so that the wire, suitably matching copper and resisting any softening and creep in fixtures that might lead to loosening. Torsion testing and TEM showed that considerably strength at 200 - 300 °C was due to the particles pinning the dislocations, whereas above 400 °C, the dislocations could by-pass the particles to give larger subgrains, lower flow stress and higher ductility [81,84,85]. Multistage isothermal tests with various interpass times showed only minor decreases in strength over some dozen passes, with holds of as much as 40 s up to 400 °C without noticeable change in subgrain size. Rolling schedules with 5 passes of 0.2, from 500 to 200 °C showed complete absence of SRX in intervals of 20s or 40s; rising pass flow stresses were less than those in isothermal steady state and associated with larger subgrains (Figure 3) [80,82,83,86-88].

Superplastic deformation (SRPD) has been induced in some precipitation alloys by a thermo-mechanical treatment of severe warm rolling with some recovery between passes, examples are Supral Al-Cu-Mg [89,90] are Al-10 Mg [91,92]. It was discovered that, in the initial superplastic straining, the fine cell structure enlarged with rising boundary misorientation resulting in continuous cDRX to fine grains that provided high ductility. Multistage torsion testing was applied to Al-Li alloys to develop a suitable dense substructure and then surveyed for SRPD in one torsion trial [88,93-95]. The alloys were given 6 stages in the range 250 - 350 °C at  $1 s^{-1}$ , with a little time between for SRV. The temperature was then raised to 450 - 550 °C and torsion conducted in 10 short bursts in steps rising from  $10^{-4}$  to  $5 \times 10^{-3} s^{-1}$ ; SRPD was confirmed from development of strain rate exponents greater than 0.4. TEM confirmed that cellular size increased, developing boundaries  $>15^\circ$ . In similar tests on 5083, SRX occurred due to particle-stimulated nucleation during rise in  $T$  with weaker SRPD [76].

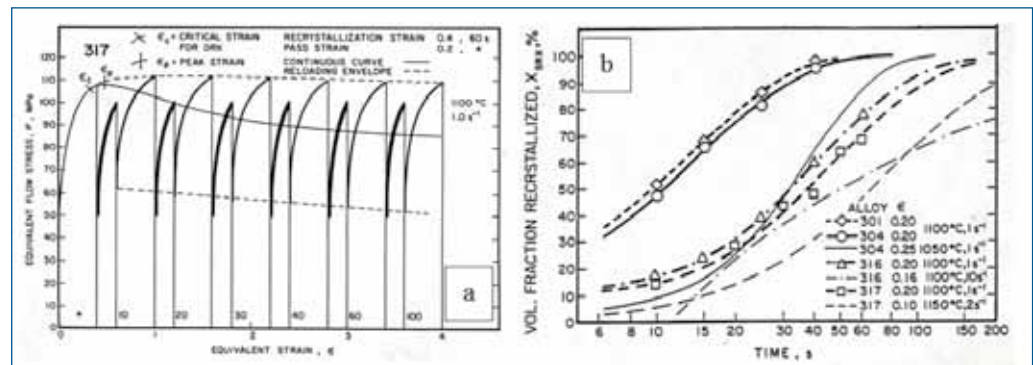
A multistage program was developed for 99.9Al and Al-5Mg (to determine the effects of Mg) with  $T$  declining 500 to 300 °C, total strain of 4.6, but with 3 combinations: a) 17 equal passes,  $\epsilon_i = 0.2$ ,  $t_i = 90$  s; b) 9 passes,  $\epsilon_i = 0.46$ , 187s; and c) 5 passes  $\epsilon_i = 0.92$ , 360s. All had slight adjustment in last pass so  $\Sigma\epsilon_i = 4.6$  and  $\Sigma t_i = 1440$  [89,97-

101]. For Al, considerable SRX ( $>80\%$ ) took place after: a) the first 3  $\Sigma\epsilon = 0.6$  (90s) of 17 passes; b) first 3  $\Sigma\epsilon = 1.8$  (187s) of 9 passes, and c) first 3  $\Sigma\epsilon = 2.76$  (360 s) of 5 passes. For Al-5Mg, SRX was more extensive, occurring after: a) first 9 of 17 passes,  $\Sigma\epsilon = 1.8$ ; b) first 7 of 9 passes  $\Sigma\epsilon = 3.22$  and c) first 4 of 5  $\Sigma\epsilon = 3.68$  [88,97]. In comparison with the isothermal flow stresses, the Al was less (25 MPa compared to 35 MPa at end), whereas the Al-5Mg had no decrease in the pass flow curves compared to the isothermal ones; these results indicate that the initial flow stress in Al-5Mg is related to separating the dislocations from the Cottrell atmospheres of Mg atoms around the dislocations [48]. In the development of uniform grain structures and isotropic sheet for can drawability, notably in Al-1Mn-1Mg alloy, rolling trials were combined with plane-strain compression testing [24] to define suitable schedules for consistent products in different mill configurations [98,102,103]

## AUSTENITIC STAINLESS STEEL MULTISTAGE SIMULATIONS

In association with Atlas Specialty Steels (an independent Canadian firm with worldwide sales from 1930 to 1980), a major project was undertaken on austenitic stainless steels ( $\gamma$ -SS, 301, 304, 316 and 317) [7,43-46,49,50,54,104-111] and ferritic ones ( $\alpha$ -SS, 407, 409, 430 and 434) [51-56]. In both as-cast and for the homogenized/forged conditions, they were tested for constitutive behavior, hot ductility and microstructure development by OM, TEM and SEM-EBSI. Due to segregation of  $\alpha$ -phase in the  $\gamma$ -SS, the as-cast exhibited high stress and low ductility, whereas the homogenized had very good properties with formation of subgrains and underwent DRX and SRX; the  $\alpha$ -phase enhanced nucleation of DRX, lowering peak  $\epsilon$  but also initiated cracking [43,44]. The  $\alpha$ -SS (even as-cast) were reasonably ductile and developed a high degree of DRV without DRX [51-56]. The as-cast were rather different from duplex stainless where nucleation of DRX in  $\gamma$ -grains is constrained by the  $\alpha$ -matrix; however, similarly cracking initiates at  $\alpha$ - $\gamma$  interfaces with much lower hot ductility than  $\alpha$ -SS or  $\gamma$ -SS [58]. The quantitative effects of alloying elements on strength, ductility, subgrain size

**Fig. 4 - Isothermal multistage test (a) to determine SRX kinetics to define holding (annealing) times; the grain size of the specimen must be restored by identical intervening passes, sufficiently large to cause complete SRX, (b)**



**rate of SRX[116,120,121]. The high, hot ductility makes this possible even for tool steels that have limited ductility because of undissolved carbides [124,125].**

*Figura 4: Test multistadio isoterma ( 1100°C  $\dot{\epsilon} = 1.0s^{-1}$   $\epsilon_i = 0.2$ ) condotta con tempi di attesa crescenti per la determinazione delle cinetiche di SRX e la definizione dei tempi di attesa dell'acciaio inossidabile 317; la dimensione dei grani del campione viene ripristinata mediante passate intermedie che determinano una completa SRX ( $\epsilon_i = 0.4$ ,  $t_i = 60$  s) (a), grado di ricristallizzazione statica al variare dei tempi di attesa per acciai inossidabili 301, 304, 316, 317 (b).*

and DRX grain size were determined [7,43,49,50,54,107]. The roles of Cr and Mo over 900 to 1200°C for rates of 0.1, 1 and 4 s<sup>-1</sup> were clarified; Mo raised the hot strength and decreased the ductility with stronger dependence on T and  $\dot{\epsilon}$  [43,107]. These results were compared with published reports (40 for 304, 25 for 316/317) to define quantitatively the effects of alloying elements and some impurities [43,50,107]. Modeling of forces and power requirements in the planetary mill (24 small rolls a rotating cage, supported by large back-up rolls) showed the strong dependence on continual DRX in the 300 type (~1200°C) but none in the 400 type (~1000°C) [71].

The simulation of a bar mill rolling schedule for austenitic stainless steels included 301, 304, 316 and 317 was the conclusion of a major project on those alloys [112-123]. It progressed from the as-cast alloys to the homogenized worked ones, with determination of the hot ductility and strength and with calculation of constitutive constants; all were combined with microstructure development, both optically and in SEM. A prior series of isothermal two-stage tests was used to measure the softening with increasing delay times and thus determine the progress of SRV and SRX; these were checked against micro-structures. The whole series could be performed on one sample, if the original grain size was restored by repeating between each a suitably large pass to cause complete SRX [114,116] (Figure 4). Research of a similar nature was carried out on C/HSLA steels with extensive work to define the conditions for various products of controlled rolling [30-36,49,50,67-70].

In the multistage tests, the preheating applied to all the homogenized steels was at 1200°C and finishing at ~900°C for 17 equal stages of  $\epsilon_i = 0.2$  and interstage  $t_i = 20$  or 40 s [3,59,113-123]. The pass flow curves for such a simulation rise steadily but more rapidly in the final stages as the degree of softening between stages diminishes: for  $\dot{\epsilon} = 1$  s<sup>-1</sup>,  $t_i = 40$ s, drops from about 100% (100%, SRX) to 40% (2% SRX), but for  $\dot{\epsilon} = 0.1$ s<sup>-1</sup>  $t_i = 20$ s from 80% (30%

SRX) to none as a result of denser substructure (Figure 5). The rise in the flow curves was greater and the degree of interpass softening was less as Mo content rose in 316 and 317 steels (Figures 4,5,6). The peak flow stress in each pass was used to determine a constitutive equation ( $Q_{MHW}$ ) for each steel in that bar mill, so that flow stresses could be calculated for the commercial mill strain rates that exceeded the torsion machine rates or for slight changes in the schedule with bar size [3,59,113-123]. Some tests were terminated after different schedule arrests so that the microstructures [117,120] could be observed both optically (more elongation becoming masked by more SRX) and in SEM (reduction in average cell size (~9 μm) and increase in dislocation density). For tool steels in a similar program, austenite behavior and decomposition were altered markedly by varying alloy carbide contents [112,124, 125].

## SUMMARY

This section will pull together the underlying mechanisms and the common elements that lead to a considerable unity in behavior that facilitates comprehension, yet an amazing diversity in behaviors that permits the utilization of similar rolling processes to provide a wide range of products with specialized properties. The starting grain size has little effect as T and  $\dot{\epsilon}$  take control.

Simple continuous tests above 0.5 T<sub>M</sub> to desired strain or failure show that dynamic recovery DRV reduces flow stress to a steady value and greatly raises ductility compared to cold working. The hot strength becomes dependent only on the subgrain size (SGB spacing rises as T↑ $\dot{\epsilon}$ ↓ and is much less than in cold working, generally raising the ductility. [11-13,16,47,63]

In Al alloys and  $\alpha$ -Fe alloys [51-57], DRV continues to high strains but due to GB serrations (defined by SGB interactions), grains become shorter but never thinner than

**Fig. 5 - Multistage tests on homogenized forged 316, 317, 304 with  $\dot{\epsilon}_i = 0.2$ ,  $\dot{\epsilon}_i = 1.0$  or  $0.1 \text{ s}^{-1}$ , declining  $T_i$  and  $t_i = 20 \text{ s}$ : a) pass flow curves with values for individual isothermal tests and b) the fractional softening in each interval declines to about 40%, being larger for 1 than  $0.1 \text{ s}^{-1}$ . When cali-brated against optical fraction SRX, it reaches  $< 5\%$  after the 8th to 12th pass [114-117,120,121].**

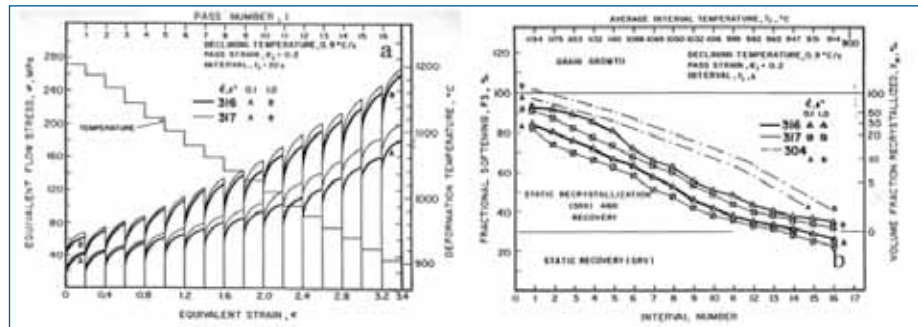


**Figura 5: Test multistadio su acciai 316, 317 e 304 omogeneizzati a  $\dot{\epsilon}_i = 0.2$ ,  $\dot{\epsilon}_i = 1.0$  o  $0.1 \text{ s}^{-1}$ ,  $T_i$  decrescenti e  $t_i = 20 \text{ s}$ : curve di flusso isoterme (a). Il softening si riduce al ridursi della SRX ed è sempre superiore per le prove effettuate alla massima velocità di deformazione (b).**

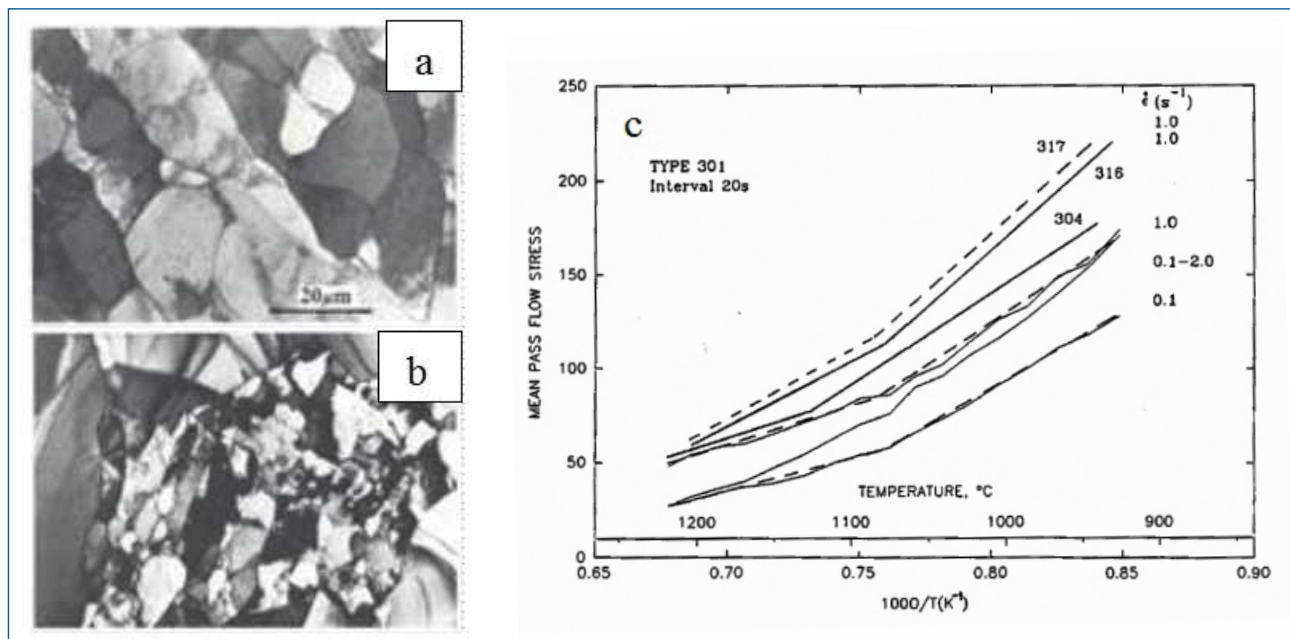


**Fig. 6 - TEM showing subgrain sizes of 317 stainless steel: a)  $1100^\circ\text{C}$ ,  $1.0\text{s}^{-1}$ ,  $4 \mu\text{m}$  and b)  $900^\circ\text{C}$ ,  $1.0 \text{ s}^{-1}$ ,  $1.4 \mu\text{m}$ ; SRX grains at edges. (c) Mean pass flow stress plotted against  $1000/T \text{ (K}^{-1}\text{)}$  for 301 at  $\dot{\epsilon} = 1.0, 0.1$  and  $0.1-2.0 \text{ s}^{-1}$  and for 304, 316, 317 at  $1.0 \text{ s}^{-1}$ . For 304, 301 dashed upward kinks indicate TNR (no SRX below it to right) (for 316, 317 partial to no SRX [43,109,114,121].**

**Figura 6: Micrografie TEM per l'acciaio inossidabile 317 dopo torsione a  $1100^\circ\text{C}$  e  $1,0 \text{ s}^{-1}$ , (dimensione dei sottograni uguale a  $4 \mu\text{m}$ ) (a) e a  $900^\circ\text{C}$  e  $1,0\text{s}^{-1}$  (dimensione dei sottograni uguale a  $1,4 \mu\text{m}$ ) (b) in cui si evidenzia una riduzione della dimensione dei sottograni al decrescere della  $T$  di prova. Valori degli sforzi di picco Vs  $1000/T$  per gli acciai 304,316 e 317 a  $1,0\text{s}^{-1}$  e per l'acciaio 301 a  $\dot{\epsilon} = 1,0, 0,1$  e  $0,1-2,0 \text{ s}^{-1}$ . I tratteggi indicano la  $T$  limite per la ricristallizzazione statica (assenza totale di ricristallizzazione statica per gli acciai 304 e 301, ricristallizzazione statica parziale o assente per gli acciai 316 e 317 [43,109,114,121]).**

subgrain size with the texture remaining almost the same as for lower strains and for cold working [6,7,11-16,27,73]. In annealing, static recovery SRV occurs more extensively resulting in larger SRX grains after longer times than for metal cold worked to same strain.

In the case of  $\gamma$ -steel (also for Cu and Ni alloys) with lower dislocation mobility, the smaller subgrains with denser SGB give rise to dynamic recrystallization DRX, leading to new grains (stress peak and softening to steady state) [4,6-8,10,11,17,18,27]  $\gamma$ -SS[42-46,104-109]. Depending on

$T$  and  $\dot{\epsilon}$ , these metals develop a substructure in the DRX grains, establishing an average size  $d_s$  controlling stress  $\sigma_s$  (similitude to DRV) and a grain size  $D_s$ . The texture differs from that after cold working or SRX [18].

In multistage deformation, the intervals between passes are the same as short annealing bursts at  $T_D$  and can be measured by the stress drop shown on reloading. SRV and SRX change microstructures at intervals considerably different from quenching and reheating that enlarges the substructure [37,38]. In rolling schedule simulations, the

pass strains are  $\epsilon_i \approx 0.2 < 0.25$  at constant  $T_i$  and with  $\Delta T$  achieved in intervals  $t_i \sim 20s$ . The drops in reload stress  $\sigma_{R(i+1)}$  with rising delay  $t_i$  provide evidence of SRV or SRX. In Al alloys,  $\alpha$ -Fe and  $\alpha$ -SS that commonly undergo only SRV, so that on reloading, the initial stress  $\sigma_{R(i+1)}$  is possibly lower than on unloading  $\sigma_{Mi}$  but is usually higher than isothermal  $\sigma_{Y(Ti+1)}$  and progresses towards  $\sigma_{S(Ti+1)}$  [86-88,97-103]. However, if there is Cottrell atmosphere pinning of dislocations, the  $\sigma_{R(i+1)} = \sigma_{Y(Ti+1)}$  as observed in Al-5Mg alloys, having about 4 times the strength and dislocation density of Al; SRX is much more prevalent [48,98,99]. In the breakdown rolling 1200 - 1000 °C for  $\gamma$ -C/HSLA-steels, there is complete SRX during intervals so that the  $\sigma_{R(i+1)}$  equals yield  $\sigma_{Y(Ti+1)}$  for the new grain size at interval end [29,49,50,65-70]. In controlled rolling of C/HSLA steels (if particles are completely dissolved), the SRX grain size usually decreases. However, if SRX is only partial, the  $\sigma_{Ri}$  rises more rapidly as  $T_D$  declines due to the retained substructures; there is a sharp rise in the slope of  $\sigma_{Ri}$  versus  $1/T$  marking the no recrystallization  $T_{NR}$ . In controlled rolling of  $\gamma$ -steels to decrease the ferrite grain size [29,49,50,67-70], the refinement is more successful for pancaked austenite that has  $d_s$  and  $D_s$  that speed up and refine the nucleation [32-38]. This is ensured by additions of ~0.3% Nb that precipitates as NbCN during continuous rolling below  $T_{NR}$  that prevents nucleation [29,49,50,67-70]. The required low T may be achieved by holding coils off-line for a period allowing other coils to pass through the break down mill. Moreover after the continuous mill, the strip must be rapidly cooled to ensure complete transformation to refined  $\alpha$ -Fe before coiling where cooling becomes very slow [29,49,50,67-70]. Multistage simulations can be performed for the following objectives:

- Ascertain what is happening at each stage of plant schedule, such as grain size. The  $T_i$ ,  $\xi_i$  of the model can be altered to achieve microstructures corresponding to the rolling;
- Determine at what stage precipitates form, their size and distribution;
- Expose internal cracks and their origin and location in GB segregation, particle type; dependence on chilling, stress concentrations, etc.;
- Once the simulation has been matched to the plant, optimize the plant behavior through variations;
- Vary minor element levels to find improvement and optimize homogenization treatments;
- Select alterations to develop specific microstructures;
- Avoid occurrence of DRX or SRX by lowering rolling T, cooling more quickly, or with alloy additions that slow GB migration.

## REFERENCES

- H. J. McQUEEN, (invited, THERMEC 2009, T.Chandra, ed., Berlin) Mat. Sci. Forum, 638-642 (2010), 3380-3387.
- H.J. McQUEEN, (Steel Processing, Product & Applications, R.Asafari, ed. M S & T'09, Pittsburgh, CD pp.1283-1293.) AIST Steel Properties and Applications Conf Proc., K.O Finlay et al.,eds., AIST Warrendale, PA, (2009), pp. 515-525.
- H.J. McQUEEN, (invited, Thermec2006,Vancouver), Mat. Res. Forum, 539-543,(2006), 4397-4404.
- H.J. McQUEEN.,(ICSM, 13, Budapest, T. Ungar) Mat. Sci. Eng. A387-389, (2004), 203-208.
- H.J. McQUEEN, N.D. RYAN and E.V. KONOPLEVA, Guthrie Symp. Proc. Metallurgy, M.Isac, ed., McGill Metal Proc. Center, Montreal, (2011), pp. 205-211.
- H.J. McQUEEN, D.L. BOURELL, Inter-relation of Metal. Structure & Formability, (A.K. Sachdev, J.D. Embury, eds.) Met.Soc.AIME,Warrendale, PA, (1987), 341-368; J. Met.,39 [9] (1987), 28-35.
- H.J. McQUEEN, Thermomechanical Processing of Steel (Jonas Symposium), S. Yue, E. Essadiqi eds., Met. Soc. CIM, Montreal, (2000), pp. 323-333.
- H.J. McQUEEN, Encyclopedia of Materials: Science and Technology, Elsevier Science, Oxford, UK, (2001), pp. 2375-2381.
- H.J. McQUEEN, Proc.ICOTOM12, J.A.Szpunar,ed.,NRC Research Pub.,Ottawa,(1999),pp.836-841.
- H.J. McQUEEN, Mat. Sci. Eng., 101 (1988), 149-160.
- H.J. McQUEEN, E. EVANGELISTA, Metal. Sci. Tech., 28[1](2010), 12-21; 28[2] (2010), 25-32.
- H.J. McQUEEN, S. SPIGARELLI, M.E. KASSNER and E. EVANGELISTA, Hot And Cold Deformation And Processing Of Aluminum Alloys, CRC Press (Taylor & Francis Group), Boca Raton, FL, USA, (2011), Chapter 4, pp. 143-190.
- H.J. McQUEEN and W. BLUM, Mat. Sci. Eng., A290 (2000), 95-107.
- H.J. McQUEEN and W. BLUM. Aluminium Alloys, Physical and Mechanical Properties ICAA6, T. Sato, ed. Japan Inst. Metals, 1998, pp. 99-112.
- G. AVRAMOVIĆ-CINGARA and H.J. McQUEEN, Aerospace Materials Manufacturing (and Repairs): Emerging Techniques, Met. Soc. CIM Montreal, M. Jahazi, et al., eds., 2006, pp. 173-186.
- H.J. McQUEEN, E. EVANGELISTA, M. CABIBBO and G. AVRAMOVIĆ-CINGARA, Can. Metal. Quart., 47, (2008), 71-82.
- H.J. McQUEEN, C.A.C. IMBERT, (ISPMA 9, Prague, F. Chmelik), J. Alloys Compounds, 378 [1,2], (2004), 35-43.
- L. GAVARD, F. MONTHILLET and H.J. McQUEEN, Proc. ICOTOM 12, J.A. Szpunar, ed., NRC Research Pub., Ottawa (1999), pp. 878-883.
- W.K.V. GALE, The British Iron and Steel Industry, David & Charles, Newton Abbot, (1967).
- F. HABASHI, ed., A History of Metallurgy, Metallurgie Extractive, Quebec, (1994).
- R.D. Doherty, D.A. Hughes, F.J. Humphreys, J.J. Jonas, D. Juul-Jansen, M.E. Kassner (editor), W.E. KING, T.R. MCNELLEY, H.J. McQUEEN and A.D. Rollett, Mat. Sci. Eng., 238 (1998), 219-274.
- H.J. McQUEEN and J.J. JONAS, Metal Forming: Interrelation Between Theory and Practice (AIME Symposium, 1970), Plenum Press, New York, 1971, pp. 393-428.
- E. EVANGELISTA, N.D. RYAN and H.J. McQUEEN, Metal. Sci. Tech., 9, 1991, pp. 75-92.
- H.J. McQUEEN, S. SPIGARELLI, M.E. KASSNER AND E. EVANGELISTA, Hot And Cold Deformation And Processing Of Aluminum Alloys, CRC Press (Taylor & Francis Group), Boca Raton, FL, USA, (2011), Chapter 3, pp. 53-86.
- H.J. McQUEEN, (ICSM 1, Tokyo) Trans. Japan Inst. Metals, 9 suppl., (1968), 170-177.
- H.P. IMMARIGION and H.J. McQUEEN, Can. Met. Quart., 8 (1969), 25-34.
- H.J. McQUEEN and H. MECKING, Z. Metallkde, 78 (1987), 387-395.
- S.R. Goodman and H. Hu, Trans. Met. Soc. AIME, 230(1964), 1413-1419; 233 (1965), 103-110.
- C. M. SELLARS, Thermomechanical Processing of Steel (Jonas Symposium), S. Yue, E. Essadiqi eds., Met. Soc. CIM, Montreal, (2000), pp. 3-19.
- E.V. KONOPLEVA, V.M. KHELESTOV, H.J. McQUEEN, Keynote Phase Transformation During Thermal-Mechanical Processing of Steel, E.B.Hawbolt, S.Yue, eds., Met. Soc. CIM, 1995, pp. 243-258.
- V.M. KHELESTOV, E.V. KONOPLEVA and H.J. McQUEEN, Mat. Sci. Tech., 14, 1997, 783-792.
- V.M. KHELESTOV, E.V. KONOPLEVA and H.J. McQUEEN, Can. Metal. Quart., 37, 1998, 75-89.
- H.J. McQUEEN, E.V. KONOPLEVA and V.M. KHELESTOV, Steel For Fabricated Structures, R.I. Asfahani, R.L. Bodnor, eds., ASM Int., Metals Park, OH, (1999), pp. 172-179.
- H.J. McQUEEN, E.V. KONOPLEVA, and V.M.KHELESTOV, Hot Workability of Steels and Light Alloys-Composites, H.J. McQUEEN, E.V. Konopleva and N.D. Ryan (eds.), Met. Soc. CIM, Montreal, 1996, pp. 349-356.
- H.J. McQUEEN, E.V. KONOPLEVA, C.A.C. IMBERT and V.M. KHELESTOV, Thermomechanical Processing: Mechanics, Microstructure, Control, E.J.Palmiere, et al., eds., Sheffield University, (2003), pp.368-373.
- V.M. KHELESTOV, H.J. McQUEEN and E.V. KONOPLEVA, Advanced Steels, J. Szpunar and H. Li, eds., Met. Soc. CIM Montreal, (2006), pp. 83-97.
- T. SHEPPARD, M.A. ZAIDI, P.A. HOLLINSHEAD and N. RAGUNATHAN, Microstructural Control in Al Alloy Processing, H.Chia, H.J. McQUEEN, eds., TMS-AIME, Warrendale, PA, (1985), pp. 19-43.
- P.A. Hollinshead and T. Sheppard, Mat. Sci. Tech., 3 (1987), 1019-1024.
- M.R. van der WINDEN, Laboratory Simulation and Modelling of the Breakdown Rolling of AA 3104, Ph.D. Thesis, Univ. Sheffield, Corus Technology BV, Netherlands (1999).
- H.J. McQUEEN and J.J. JONAS, The Plastic Deformation of Materials, R.J. Arsenault, ed., Academic Press, New York, 1975, pp. 393-493.
- J. McQUEEN, S. SPIGARELLI, M.E. KASSNER and E. EVANGELISTA, Hot And Cold Deformation And Processing Of Aluminum Alloys, CRC Press (Taylor & Francis Group), Boca Raton, FL, USA, (2011), Chapter 8, pp. 267-300.



42. L. FRITZMIER, M. LUTON and H.J. McQUEEN, Strength of Metals and Alloys, (ICSM 5, Aachen), P. Haasen et al. eds., Pergamon Press, Frankfurt, (1979), 1, pp. 95-100.
43. N.D. RYAN and H.J. McQUEEN, Stainless Steels, Inst. Metals, London, (1988), pp. 498-507.
44. E. EVANGELISTA, N.D. RYAN and H.J. McQUEEN, Metal Sci. Tech., 5[2], (1987), 50-58.
45. N.D. RYAN and H.J. McQUEEN, J. Mat. Proc. Tech., 21 1990, pp. 177-199.
46. N.D. RYAN and H.J. McQUEEN, High Temperature Technology, 8 (1990), 27-44, 185-200.
47. H.J. McQUEEN, S. SPIGARELLI, (ISPMA, 2005, Prague), Mater. Sci. Eng., A 462 (2007), 37-44.
48. H.J. McQUEEN and W. BLUM, Aluminium 80, (2004), 1151-1159, 1263-1270, 1347-1355.
49. H.J. McQUEEN, S. YUE, N.D. RYAN and E. FRY, Advanced Materials and Technologies, L.A. Dobrzanski, ed., Silesian Tech. Univ., Gliwice, Poland, 1995, pp. 295-332.
50. H.J. McQUEEN, S. YUE, N.D. RYAN and E. FRY, J. Mat. Proc. Tech. 53, (1995), 293-310.
51. H.J. McQUEEN, E. EVANGELISTA, P. MENGUCCI, N.D. RYAN and J. BOWLES, Application of Stainless Steels '92, H. Nordberg, J. Bjorklund, (eds.), Jernkontoret, Stockholm, (1992), pp. 924-933.
52. H.J. McQUEEN, N.D. RYAN, E. EVANGELISTA, X. XIA, 34th Mechanical Working and Steel Processing Conf. Proc., Iron Steel Soc., Warrendale, PA, (1993), 30, pp. 101-107.
53. N.D. RYAN, C. IMBERT and H.J. McQUEEN, Strip Casting, Hot and Cold Working of Stainless Steels, (Met. Soc. CIMM Conf., Quebec City), N.D. Ryan, A. Brown and H.J. McQUEEN, eds., CIMM, Montreal, (1993), pp. 165-180.
54. H.J. McQUEEN, N.D. RYAN, R. ZARIPOVA and K. FARKHUTDINOV, Proc. 37 Mech. Working and Steel Processing Conf. (1995), Iron and Steel Soc., AIME, Warrendale PA, 1996, pp. 883-894.
55. E.V. KONOPLEVA, M. SAUERBORN, H.J. McQUEEN, N.D. RYAN and R.G. ZARIPOVA, Strength of Materials, (ICSM 11, Prague, P. Lukas) Mat. Sci. Eng. A234-236, (1997), pp. 826-829.
56. N.D. RYAN and H.J. McQUEEN, Innovative Technologies For Steel (G. Heffernan Symp.), J. Guerard, E. Essadiqi, eds., Met. Soc. CIM, Montreal, (2001), pp. 291-306.
57. ANI SHEN and H.J. McQUEEN, Canadian Metal. Quart., 48 (2009), 207-218.
58. E. EVANGELISTA, H.J. McQUEEN, M. Niewczasz, M. Cabibbo, Can. Met. Quart., 43 (2004), 339-353.
59. H.J. McQUEEN and E. EVANGELISTA, Super-High Strength Steels, A. J. Deardo et al. eds., Assoc. Italiana Metal., Milan 2010, electronic Plenary, Index paper 10 (22 pages).
60. H.J. McQUEEN, YONG LI, I. RIEIRO, M. CARSI, O.A. RUANO, TMS 2011 Supl. Proc. Vol. 2: Material Processing, Characterization, Computation, Modeling, (TMS electronic) John Wiley & Sons, Hoboken NJ, (2011), pp. 921-929.
61. S. FULOP, K.C. CADIEN, M.J. LUTON and H.J. McQUEEN, J. Test Evaluation, 1977, 5, 419-26.
62. H.J. McQUEEN and N.D. RYAN, Mat. Sci. Eng., A322, (2002), 43-63.
63. H.J. McQUEEN and J.E. HOCKETT, Met. Trans., 1, (1970), 2997-3004.
64. F.X. ZHU, C. LIU, G.Z. CHUI and D.F. GAO, Acta Metal. Sinica, 13 (2000), 335-341.
65. J. SANKAR, D. HAWKINS and H.J. McQUEEN, Met. Tech., 1979, 6, 325-331.
66. W. KNUDSEN, J. SANKAR, H.J. McQUEEN, J.J. JONAS and D. HAWKINS, Hot Working and Forming Processes, Proc. Sheffield Conf., Metals Society, London, 1980, 51-56.
67. I. WEISS, J.J. JONAS, P.J. HUNT and G.E. RUDDLE, Proc. Int. Conf. on Steel Rolling, I.S.I.J., Tokyo, (1980), pp. 1225-1236.
68. M. G. AKBEN, I. WEISS and J.J. JONAS, Acta Metall., 29 (1981), 111.
69. B. BACROIX, C. G'SELL, M.G. AKBEN and J.J. JONAS, Acta Metall., 31 (1983), 619-629.
70. H.J. McQUEEN, M. G. AKBEN and J.J. JONAS, Microstructural Characterization by Non-Microscopic Techniques, (N.H. Anderson, eds.) Riso Natl. Lab, Roskilde, Denmark, 1984, 397-404.
71. N.D. RYAN, H.J. McQUEEN, Proc. 4<sup>th</sup> Intl. Steel Rolling Conf. (France), 1987, pp. F.17-1-F.17.9.
72. C. ROSSARD, Métaux Corros, Inds., 35 (1960), 102-115, 140-153, 190-205.
73. J.K. SOLBERG, H.J. McQUEEN, N. RYAN, E. NES, Phil. Mag., 60, (1989), 447-471, 473-485.
74. H.J. McQUEEN and O.C. CELLIERI, Can. Metal. Quart., 35, (1996), 305-319; 36, (1997), 73-86.
75. H.J. McQUEEN, S. SPIGARELLI, M.E. KASSNER AND E. EVANGELISTA, Hot And Cold Deformation And Processing Of Aluminum Alloys, CRC Press (Taylor & Francis Group), Boca Raton, FL, USA, (2011), Chapter 14, pp. 461-522.
76. H.J. McQUEEN, E.V. KONOPLEVA, H. FARAH and E. HERBA, Design, Manufacturing and Application of Composites (CANCOM 2001), S.V. Hoa, A. Johnston, J. Deneault, eds., Technomic Pub., Westport, CT., (2001), pp. 435-444.
77. D.S. SALONINE and H.J. McQUEEN, Light Metals 2005 Métaux Legers, J.-P. Martin, (ed.), Met. Soc. CIM, Montreal (2005), 305-317.
78. H.J. McQUEEN, Hot Deformation of Aluminum Alloys, Detroit, Oct. 1990, T.G. Landon and H.D. Merchant, eds., TMS-AIME, Warrendale, PA, 1991, pp. 105-120.
79. E. EVANGELISTA, H.J. McQUEEN and E. CERRI, Modelling of Plastic Deformation and its Engineering Applications, S.I. Andersen, et al., eds., Roskilde, DK, (1992), pp. 265-270.
80. H.J. McQUEEN, H. CHIA, E.A. STARKE, Microstructural Control in Al Alloy Processing, (H. Chia, H.J. McQUEEN, eds.) Met. Soc., AIME, Warrendale, PA, 1986, 1-18; J. Met., 38 [4] (1986), 19-24.
81. H.J. McQUEEN, S. SPIGARELLI, M.E. KASSNER AND E. EVANGELISTA, Hot And Cold Deformation And Processing Of Aluminum Alloys, CRC Press (Taylor & Francis Group), Boca Raton, FL, USA, (2011), Chapter 5, pp. 143-190.
82. G. AVRAMOVIC-CINGARA, H.J. McQUEEN, I.SZKRUMELAK, K. CONROD, Microstruct Sc., 17 (1989), 375-392.
83. A. CINGARA, H.J. McQUEEN, G. AVRAMOVIC-CINGARA, Scripta Metal. Mat., 30, (1994), 1437-1442.
84. H.J. McQUEEN, (Keynote, Asia Pacific Conf. Mat. Proc.), J. Mat. Proc. Tech., 37, (1993), 3-36.
85. G. AVRAMOVIC-CINGARA and H.J. McQUEEN, Aluminium, (1994), 70, pp. 214-219.
86. H.J. McQUEEN, G. AVRAMOVIC-CINGARA P. SAKARIS and A. CINGARA, Proc. 3rd Intl. SAMPE Metals Conf., (Toronto), (1992), pp. M192-M206.
87. G. AVRAMOVIC-CINGARA, K. CONROD, A. CINGARA and H.J. McQUEEN, Light Metals Processing and Applications, C. Bickert, ed., Met. Soc., CIMM, Montreal, (1993), pp. 495-510.
88. H.J. McQUEEN and M.E. KASSNER, Light Weight Alloys for Aerospace Application, K. Jata, et al., eds., TMS-AIME, Warrendale, PA, (2001), pp. 63-75.
89. H.J. McQUEEN, S. SPIGARELLI, M.E. KASSNER and E. EVANGELISTA, Hot And Cold Deformation And Processing Of Aluminum Alloys, CRC Press (Taylor & Francis Group), Boca Raton, FL, USA, (2011), Chapter 12, pp. 407-436.
90. B.M. WATTS, M.J. STOWELL, B.L. BAIKIE, D.G.E. OWEN, Met. Sci., 10, (1976), 189-197, 198-205.
91. S.J. HALES, T.R. MCNELLEY and H.J. McQUEEN, Met. Trans., 22A, (1991), 1037-1042.
92. H.J. McQUEEN, S. SPIGARELLI, M.E. KASSNER and E. EVANGELISTA, Hot And Cold Deformation And Processing Of Aluminum Alloys, CRC Press (Taylor & Francis Group), Boca Raton, FL, USA, (2011), Chapter 13, pp. 437-460.
93. G. AVRAMOVIC-CINGARA, K.T. AUST, D.D. PEROVIC, G. PALUMBO and H.J. McQUEEN, H.J. McQUEEN, N.D. Ryan, E.V. Konopleva and X. Xia, (Engineering Aspects Of Grain Boundary and Interface Science), Can. Metal. Quart., (1995), 34, pp. 265-273. *Best Materials Science Paper CIM, 1995.*
94. G. AVRAMOVIC-CINGARA, D.D. PEROVIC, H.J. McQUEEN, Met. Mat. Trans A, 1996, 27A, 3478-3490.
95. G. AVRAMOVIC-CINGARA, H.J. McQUEEN, D.D. PEROVIC, Can. Met. Quart., 43, (2004), 193-202.
96. H.J. McQUEEN, W. Blum and Q. Zhu, Superplasticity in Advanced Materials (ICSAM, '94 (Moscow), T.G. Langdon ed. Trans. Tech., Pub. Switz., 1994, pp. 193-200.
97. I. Poschmann and H.J. McQUEEN, Z. Metallkde. 87 (1996), 349-356; 88 (1997), 14-22.
98. H.J. McQUEEN, S. SPIGARELLI, M.E. KASSNER and E. EVANGELISTA, Hot And Cold Deformation And Processing Of Aluminum Alloys, CRC Press (Taylor & Francis Group), Boca Raton, FL, USA, (2011), Chapter 15, pp. 523-544.
99. H.J. McQUEEN and I. POSCHMANN, THERMEC '97 (Woolongong, Australia) T. Chandra, ed., TMS-AIME, Warrendale, PA, (1997), Vol. 1, pp. 951-957.
100. H.J. McQUEEN Hot Deformation of Al Alloys T.R. Bieler et al., eds., TMS-AIME Warrendale PA, 1998, pp. 383-396.
101. H.J. McQUEEN, Advances in Metallurgy of Aluminum Alloys (J.T. Staley Symp.), M. Tiryakoglu, ed., ASM Intl., Materials Park, OH, (2001), pp. 351-360.
102. J. HIRSCH, K. KARHAUSEN and R. KOPP, Al Alloys Physical Mechanical Properties, ICAAA, T. Sanders and E.A. Starke, eds., Georgia Inst. Tech., Atlanta (1994), pp. 476-483.
103. J. HIRSCH, Thermec '97, T. Chandra and T. Sakai, eds., TMS-AIME, Warrendale, PA, (1998), pp. 1083-1094.
104. N.D. RYAN, H.J. McQUEEN and J.J. JONAS, Can. Met. Q., 1983, 22, 369-78.
105. N.D. RYAN, E. EVANGELISTA and H.J. McQUEEN, Innovation for Quality, (Bologna Conf.), Assoc. Ital. Metal, Milano, (1988), pp. 215-234. *Metallurgia Italiana*, 81 (1989), 119-131.
106. H.J. McQUEEN, J. BOWLES and N.D. RYAN, Microstruct Sc., 17 (1989), 357-373.
107. H.J. McQUEEN and N.D. RYAN, High Temp. Mat. Proc., 12 (1993), 87-96.
108. H.J. McQUEEN, A. CINGARA and N.D. RYAN, Application of Stainless Steels '92, H. Nordberg, J. Bjorklund, (eds.), Jernkontoret, Stockholm, (1992), pp. 904-913.
109. H.J. McQUEEN, N.D. RYAN and E. EVANGELISTA, Application of Stainless Steels '92, H. Nordberg, J. Bjorklund, (eds.), Jernkontoret, Stockholm, (1992), pp. 924-932, pp. 914-923.
110. H.J. McQUEEN, X. XIA, Y. CUI, B. LI, Q. MENG, N.D. RYAN, Strip Casting, Hot and Cold Working of Stainless Steels, N.D. Ryan, A. Brown, H.J. McQUEEN, eds., CIMM, Montreal, (1993), pp. 117-129, 181-192.
111. H.J. McQUEEN, E. EVANGELISTA, E.V. KONOPLEVA and N.D. RYAN, Processes & Materials Innovation, Stainless Steel 1993, (Florence), W. Nicodemi, ed., Assoc. Ital. Metal., Milan, (1993), 2, pp. 289-302; 3, pp. 291-296.
112. N.D. RYAN and H.J. McQUEEN, J. Mech. Working Tech., 12, (1986), 279-296, 323-349.
113. H.J. McQUEEN, N.D. RYAN and E. FRY, Mathematical Modelling of Hot Rolling of Steel, S. Yue, ed., Can. Inst. Mining Metal., Montreal, 1990, pp. 269-280.
114. N.D. RYAN, and H.J. McQUEEN, Materials Forum (Australia), 14, (1990), 283-295.
115. N.D. RYAN and H.J. McQUEEN, Can. Met. Quart., 30, (1991), 113-124.
116. N.D. RYAN and H.J. McQUEEN, Mat. Sci. Tech., 7, (1991), 815-828.
117. E. EVANGELISTA, H.J. McQUEEN, N.D. RYAN and J. BOWLES, Stainless Steels, 1991 (Chiba), Iron Steel Inst. Japan, Tokyo, 1991, pp. 842-849.
118. N.D. RYAN and H.J. McQUEEN, J. Mat. Proc. Tech., 36, (1993), 103-123.
119. N.D. RYAN, E. EVANGELISTA and H.J. McQUEEN, Recrystallization '92, M. Fuentes, J. Gil Sevillano, eds., TransTech Pub., Switzerland (Mat. Sci. Forum, 113-115, (1993), 515-520.
120. N.D. RYAN and H.J. McQUEEN, Aspects of High Temperature Deformation and Fracture in Crystalline Solids, (JIMS 7), Y. Hosoi, ed., Japan Inst. Metals, Sendai, (1993), pp. 59-65.
121. H.J. McQUEEN and N.D. RYAN, Strip Casting, Hot and Cold Working of Stainless Steels, N.D. Ryan, A. Brown and H.J. McQUEEN, eds., CIMM, Montreal, (1993), pp. 91-106.
122. E.V. KONOPLEVA, H.J. McQUEEN and N.D. RYAN, Hot Workability of Steels and Light Alloys-Composites, H.J. McQUEEN, E.V. Konopleva and N.D. Ryan (eds.), Met. Soc. CIM, Montreal, 1996, pp. 431-442.
123. H.J. McQUEEN, N. D. RYAN and R.G. ZARIPOVA, Ultra-Fine Structured Steels, E. Essadiqi and J. Thomson, eds., Met. Soc. CIM, Montreal, (2004), pp. 55-67.
124. C. IMBERT and H. McQUEEN, Hot Workability of Steels and Light Alloys-Composites, H.J. McQUEEN, E.V. Konopleva, N.D. Ryan (eds.), Met. Soc. CIM, Montreal, 1996, pp. 451-458, 459-466.
125. C.A.C. IMBERT and H.J. McQUEEN, Mat. Sci. Eng. A313, (2001), 88-103, 104-116.

## Laminazione a caldo: caratterizzazione microstrutturale e meccanica di leghe ferrose e non ferrose mediante simulazioni

**Parole chiave:** Laminazione a caldo di leghe di Al - Acciai inossidabili - Acciai al carbonio - HSLA - Acciai per utensili - Simulazioni di laminazione mediante prove di torsione a caldo - Microstruttura.

Le dimensioni, la velocità e la complessità degli impianti di laminazione sono andate crescendo negli anni grazie agli studi sulla meccanica di processo. Tuttavia, sia per il calcolo delle forze di laminazione che per evitare difettosità di prodotto, è fondamentale conoscere l'evoluzione microstrutturale del laminato durante ogni passata e tra una passata e l'altra. A tale scopo in questo lavoro sono state simulate laminazioni multistadio mediante prove di torsione a caldo che consentono di ottenere deformazioni importanti. Nota infatti la dipendenza dell'evoluzione microstrutturale e dei valori di tensione ( $\sigma$ ) da deformazione ( $\epsilon$ ), velocità di deformazione ( $\dot{\epsilon}$ ) e Temperatura (T) di prova per leghe di alluminio, acciai al carbonio (C Steel), acciai microalligati ad alta resistenza meccanica (High Strength Low Alloy /HSLA), acciai per utensili e acciai inossidabili austenitici e Duplex, è possibile prevederne la microstruttura in relazione ai parametri di processo sia durante la laminazione che nei tempi di attesa tra le passate e garantire quindi i requisiti di qualità dei prodotti. In particolare le simulazioni mediante prove di torsione consentono di:

- a) Determinare l'evoluzione microstrutturale in ogni fase del processo di laminazione (es. dimensione del grano) noti T e  $\dot{\epsilon}$ ;
- b) Determinare se e in quale fase del processo interviene precipitazione di seconde fasi e valutare dimensione e distribuzione delle stesse;
- c) Individuare sia la presenza di cricche che la loro distribuzione e localizzazione (in corrispondenza ad esempio di segregazione, particelle) e determinarne la causa (ciclo di raffreddamento, concentrazione di sforzi);
- d) Variare le percentuali di alliganti secondari e ottimizzare i trattamenti di omogenizzazione;
- e) Individuare le variazioni dei parametri di processo che consentono di sviluppare un'ideale microstruttura finale;
- f) Evitare la ricristallizzazione dinamica (DRX) o statica (SRX) abbassando la T di laminazione, adottando un raffreddamento più rapido o aggiungendo elementi di lega che riducano la mobilità delle dislocazioni.

Le simulazioni multistadio in combinazione con l'esame al microscopio ottico (OM) al microscopio elettronico in trasmissione (TEM) e al microscopio elettronico a scansione (SEM) hanno portato alle seguenti conclusioni per le diverse leghe considerate:

1. La deformazione a caldo delle leghe di alluminio è controllata dal recupero dinamico (DRV) che, per prove effettuate a temperature superiori a  $0.5 T_M$ , determina uno stato stazionario della tensione e incrementa la duttilità. Il valore della tensione stazionaria si riduce all'aumentare della dimensione dei sottogranuli ossia all'aumentare di T e/o al ridursi della velocità di deformazione. Dall'esecuzione di prove multistadio su lega Al-0,65Fe ricristallizzata, a T che decrescono progressivamente da 500 a 200°C durante gli intervalli di attesa tra le prove, si osserva un softening (addolcimento) crescente all'aumentare del tempo di attesa e imputabile principalmente a recupero statico (SRV). Solo per la lega Al-5Mg il softening è imputabile a ricristallizzazione statica (SRX).
2. La deformazione a caldo degli acciai inossidabili austenitici è controllata da recupero (DRV) e ricristallizzazione dinamica (DRX). Dall'esecuzione di prove multistadio isoterme a 1100°C, si osserva un addolcimento crescente all'aumentare del tempo di attesa inter-stadio dovuto a SRX. Durante prove multistadio a T decrescenti da 1200°C a 900°C e tempi di attesa costanti, la T e la velocità di prova influenzano il grado di ricristallizzazione e di softening. Velocità e/o T di prova elevate favoriscono la SRX. All'aumentare del contenuto di Mo è stata osservata una riduzione del grado di softening.
3. Prove multistadio isoterme su acciai al carbonio e HSLA a 950°C indicano che, a parità di condizioni, gli HSLA esibiscono grado di softening molto inferiore a quello degli acciai al carbonio ma che può essere incrementato aumentando sia la deformazione di prova che la velocità di deformazione.